Supporting Information

An Investigation Relevant to the Conformation of the 17-Membered Pt(d(GpG)) Macrocyclic Ring Formed by Pt Anticancer Drugs with DNA. Pt Complexes with a 'Goldilocks' Carrier Ligand

Vidhi Maheshwari, Patricia A. Marzilli, and Luigi G. Marzilli*

Department of Chemistry, Louisiana State University, Baton Rouge, Louisiana 70803

E-mail: lmarzil@lsu.edu

Conformational Features of (Et$_4$dt)Pt(d(G*pG*)) Conformers. The H8 peaks of (**Et$_4$dt**)Pt(d(G*pG*)) at 8.97 and 9.04 ppm are connected by H8-H8 NOE cross-peaks. The H8-H2′ cross-peaks are stronger than the H8-H1′ cross-peaks (Figure S1), indicating a predominantly *anti* conformation for both 3′-G* and 5′-G* nucleotides. A 5′-G* H8-H3′ NOE cross-peak and a doublet for the H1′ signal (6.39 ppm) is characteristic of an N-sugar of a 5′-G (Figure S1).[1-6] The H8 signal at 8.97 ppm, which must be the 3′-G* H8 signal, has no H8-H3′ cross-peak; the H1′ signal at 6.43 ppm is a doublet of doublets, thus indicating an S-sugar pucker. Therefore, the dominant (**Et$_4$dt**)Pt(d(G*pG*)) conformer at one week is an *anti,anti*-HH1 conformer, as observed for (**Me$_4$dt**)Pt(d(G*pG*)).

The two most downfield H8 signals at 9.23 and 9.10 ppm connected by an H8-H8 NOE cross-peak belong to the HH2 conformer (minor). The G* H8 signal at 9.10 ppm has a strong H8-H3′ cross-peak, indicating an N-sugar pucker for the 5′-G* nucleotide (Figure S1). For the 5′-G* residue, a strong H8-H2′ cross-peak and the absence of an H8-H1′ NOE cross-peak indicate an *anti* G* conformation (Figure S1). The 9.23 ppm H8 signal belongs to the 3′-G* because of the S-sugar pucker indicated by the absence of an H8-H3′ NOE cross-peak. This H8 signal has a weak NOE cross-peak to the H1′ signal and a strong NOE to the H2′ signal. Therefore, this HH2 conformer has an *anti,anti* conformation.

The upfield pair of H8 signals at 8.29 and 8.32 ppm for the (**Et$_4$dt**)Pt(d(G*pG*)) adduct has no H8-H8 NOE cross-peak, indicating that the bases of this conformer adopt the HT arrangement.[2,3,7] These upfield H8 signal positions are characteristic of the ΔHT1 conformer. The chemical shifts of these HT H8 signals are similar to those of the (**Me$_4$dt**)Pt(d(G*pG*)) ΔHT1 conformer. The H8 peak at 8.32 ppm exhibits an intraresidue H8-H3′ NOE cross-peak (Figure S1) consistent with an N-sugar pucker. Because the H1′ signal of this conformer at 6.35 ppm overlaps with H1′ signals of the other (**Et$_4$dt**)Pt(d(G*pG*)) conformers, the coupling pattern could not be determined. However, because all the d(G*pG*) adducts typically adopt a 5′-G* N-sugar pucker, we can assign the downfield H8 signal of this conformer to the 5′-G*. The presence of a strong H8-H2′ cross-peak (Figure S1) and a weak H8-H1′ cross-peak indicates an *anti* 5′-G* conformation. The presence of an intraresidue H8-H1′ NOE

cross-peak for the upfield ΔHT1 H8 signal at 8.29 ppm (which must be the 3′-G* H8) suggests that the conformation of 3′-G* is *syn*. Both the H8-H2′/H2″ and the H8-H3′ cross-peaks were absent. The doublet of doublets coupling of the 3′-G* H1′ signal (6.19 ppm) is typical of an S-sugar. Thus, this (**Et$_4$dt**)Pt(d(G*pG*)) conformer has an *anti,syn*-ΔHT1 conformation. In contrast to the H8 shifts of the (**Me$_4$dt**)Pt(d(G*pG*)) ΔHT1 conformer, the 5′-G* H8 signal for the (**Et$_4$dt**)Pt(d(G*pG*)) ΔHT1 conformer is downfield to the 3′-G* H8 signal.

For the (**Et$_4$dt**)Pt(d(G*pG*)) adduct, no H8-H8 NOE cross-peak was observed for the fourth pair of G* H8 signals at 8.66 and 8.99 ppm, indicating that the bases adopt an HT arrangement. The G* H8 signals have strong H8-H2′ cross-peaks and weak H8-H1′ cross-peaks (Figure S1), indicating an *anti* conformation for both G* nucleotides. A strong H8-H3′ NOE cross-peak for the H8 signal at 8.99 ppm and a doublet for the H1′ signal indicate an N-sugar pucker. Thus, the 8.99 ppm H8 signal was assigned to the 5′-G* residue. For the H8 signal at 8.68 ppm, an H8-H3′ cross-peak was absent, and the doublet of doublets coupling pattern indicated an S-sugar pucker. Thus, this upfield signal was assigned to the 3′-G*. This HT conformer has an *anti,anti* conformation. For the ΛHT2 conformer of the (**Et$_4$dt**)Pt(d(G*pG*)) adduct, the 5-G* H8 signal is downfield of the 3-G* H8 signal, as observed for the ΛHT2 conformer of the (**Me$_4$dt**)Pt(d(G*pG*)) adduct.

The ROESY spectrum of (**Et$_4$dt**)Pt(d(G*pG*)) (Figure S1) provides clear evidence for steric crowding. NOE cross-peaks were observed between the **Et$_4$dt** methyl signals (overlapping from 0.90 to 1.10 ppm) and the H8 signals of the HH2 3′-G*, the HH1 3′- and 5′-G*'s, and the ΛHT2 3′-G*. Also, NOE cross-peaks between the methyl signals and the H1′ sugar signals were observed. No such NOE cross-peaks were observed in the ROESY spectrum of the (**Me$_4$dt**)Pt(d(G*pG*)) adduct. The NOE cross-peaks between the G* residue and the **Et$_4$dt** carrier ligand clearly indicate that the 6/6′ Et groups are close to the Pt-bound G* residues.

For (**Et$_4$dt**)Pt(d(G*pG*)), the ^{1}H NMR signal intensities indicated that the respective distribution of the HH1, HH2, ΔHT1 and ΛHT2 conformers changed from 42%, 37%, 11%, and 10% at one week to

41%, 33%, 9% and 17% at eight weeks (Figure 8). The 17% relative abundance of the ΛHT2 conformer was considerably less than the 40% observed for the (**Me$_4$dt**)Pt(d(G*pG*)) adduct (Table 2). Evidently, the ΛHT2 conformer for (**Et$_4$dt**)Pt(d(G*pG*)) is less favored than for (**Me$_4$dt**)Pt(d(G*pG*)) because of the bulk of the Et group, a result suggesting that bulk disfavors the ΛHT2 conformer.

HPLC Analysis of (Et$_4$dt)Pt(d(G*pG*)). A one-week-old sample of the (**Et$_4$dt**)Pt(d(G*pG*)) adduct gave three HPLC peaks with RT 27.2 (42% HH2 + ΔHT1), 29.5 (44% HH1), and 31.9 (14% ΛHT2) min (Figure 7). Each (**Et$_4$dt**)Pt(d(G*pG*)) peak upon re-injection eventually gave four product peaks (RT = 27.7, 28.4, 30.0 and 32.5 min) with retention times influenced by the residual salt and attributable to ΔHT1, HH2, HH1 and ΛHT2, respectively.

For (**Et$_4$dt**)Pt(d(G*pG*)), the peaks for other conformers upon reinjection were readily observed only after two days, indicating slow redistribution in comparison to (**Me$_4$dt**)Pt(d(G*pG*)). After four days, substantial conformer redistribution was observed, with each isolated peak giving four peaks as follows: the ΔHT1 + HH2 peak gave ΔHT1 (18%), HH2 (50%), HH1 (21%) and ΛHT2 (11%); the HH1 peak gave ΔHT1 (10%), HH2 (19%), HH1 (63%), and ΛHT2 (8%); and the ΛHT2 peak gave ΔHT1 (7%), HH2 (38%), HH1 (26%), and ΛHT2 (29%). The sequence of conformer interconversion for (**Et$_4$dt**)Pt(d(G*pG*)) was thus similar to that observed for (**Me$_4$dt**)Pt(d(G*pG*)). The HH1 conformer with RT = 30.0 min converts to the ΔHT1 conformer (RT = 27.7 min), which rapidly interconverts to the HH2 conformer (RT = 28.4 min). The ΛHT2 conformer (RT = 32.5 min) converts first to the HH2 conformer, which then equilibrates to give the ΔHT1 and HH1 conformers.

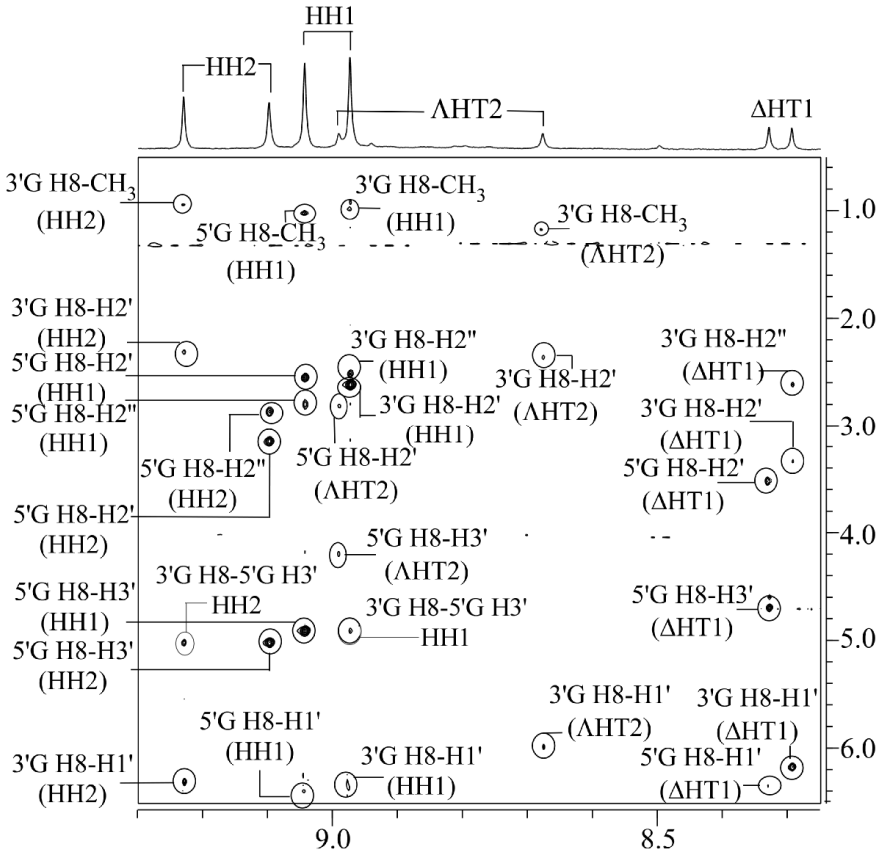

Figure S1. ROESY spectrum (700 MHz, 600 ms mixing time) of a 1-week-old (**Et$_4$dt**)Pt(d(G*pG*)) sample at pH 4.0 and 25 °C, showing G* H8-to-deoxyribose ^{1}H-^{1}H NOE cross-peaks for the HH1, HH2, and ΔHT1 and ΛHT2 conformers and G* H8-to-methyl ^{1}H-^{1}H NOE cross-peaks for the HH1, HH2 and ΛHT2 conformers.

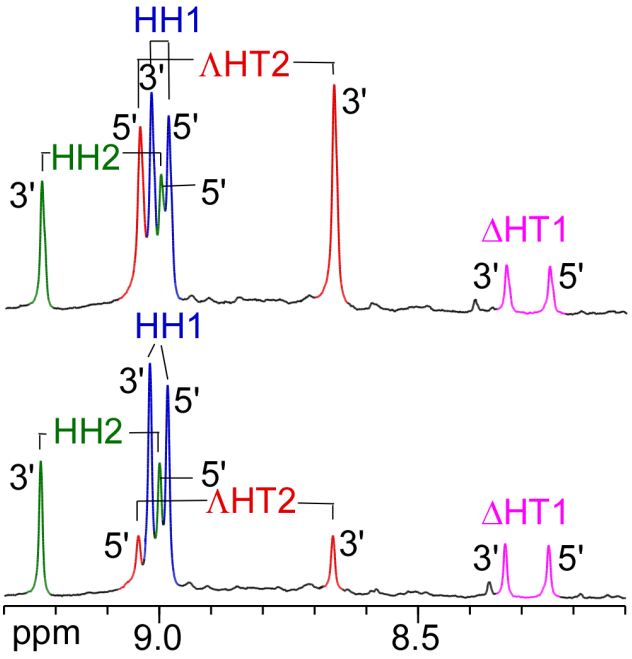

Figure S2. ^{1}H NMR spectra (400 MHz) in the H8 region for (**Me$_4$dt**)Pt(d(G*pG*)) collected at 25 °C after 1 week (bottom) and after 3 months (top) (pH 4.0, in D_2O/DMSO-d_6).

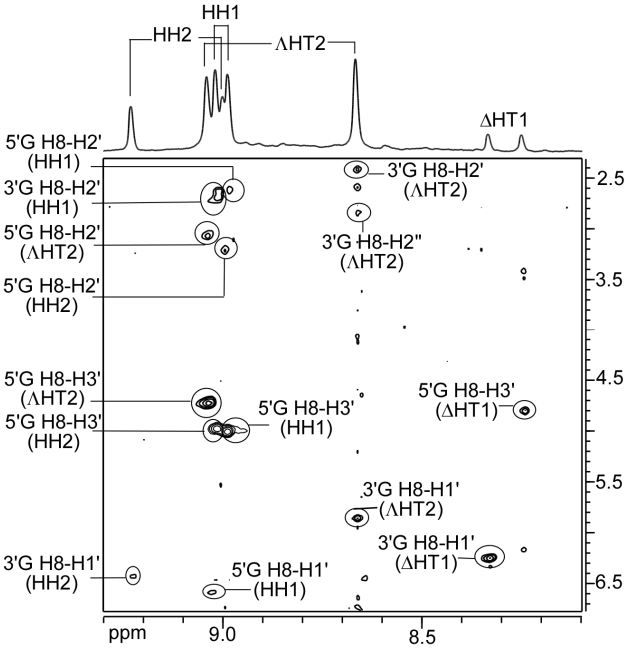

Figure S3. ^{1}H-^{1}H ROESY spectrum (400 MHz, 500 ms mixing time) of a 3-month-old (**Me$_4$dt**)Pt(d(G*pG*)) sample at pH 4.0 and 25 °C, showing G* H8-to-sugar NOE cross-peaks. In this sample, all eight H8 peak tops are resolved, including the four peaks just downfield of 9 ppm.

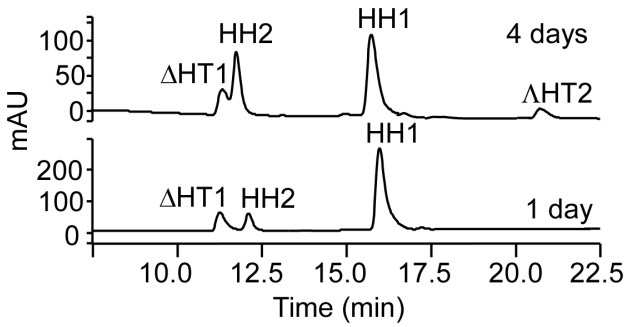

Figure S4. HPLC chromatograms of the (**Me$_4$dt**)Pt(d(G*pG*)) fraction collected at 15.7 min containing the HH1 conformer upon re-injection after 1 day (bottom) and after 4 days (top).

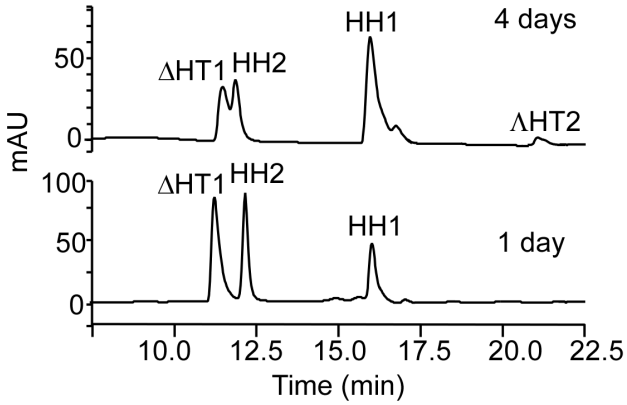

Figure S5. HPLC chromatograms of the (**Me$_4$dt**)Pt(d(G*pG*)) fraction collected at 10.8 min containing ΔHT and HH2 conformers upon re-injection after 1 day (bottom) and after 4 days (top).

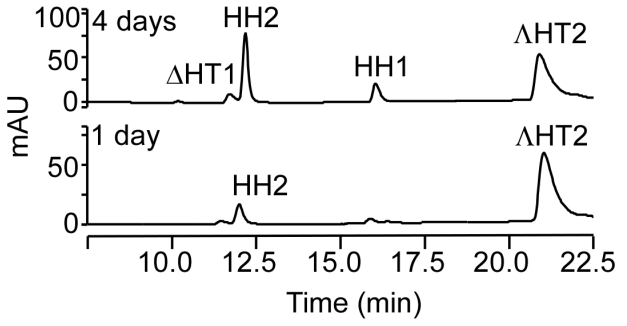

Figure S6. HPLC chromatograms of the (**Me$_4$dt**)Pt(d(G*pG*)) fraction collected at 20.3 min containing the ΛHT conformer upon re-injection after 1 day (bottom) and after 4 days (top).

Evidence for Relative Rates of Interconversion between Conformers. Although our study was designed to employ NMR methods to assess conformation and not mechanism or rates (we used, for example, 500 and 600 ms mixing times), the HPLC results obtained provide a particularly good indication of the likely pathways involved in conformer interchange. In general, it seems certain that the interchange processes are stepwise, involving rotations about one or more single bonds (including the Pt–N7 bond) in one G* residue at a time, as shown in Figure 1. Depending on whether the rotation occurs in the 5′-G* or the 3′-G* residue, one or two conformers will form from any given conformer. Until the present study, there has been no evidence to indicate which residue (5′-G* or 3′-G*) in a given conformer changes conformation more readily. We cannot rule out interconversion of HH1 and ΛHT2 completely, but we see no HPLC evidence for this isomerization, which involves the 5′-G* residue. On the other hand, HH2 can convert to ΛHT2, a process involving conformational changes of the 3′-G* residue. Under the solution conditions dictated by the isolation of the HPLC peaks, the rate of change in the size of the ΛHT2 HPLC peak is rather informative. The ΛHT2 HPLC peak preferentially forms the HH2 HPLC peak. The HH2 conformer is less stable than the HH1 conformer (Table 2), and thus this ΛHT2 to HH2 conversion is a kinetically controlled process. The 3′-G* residue of the ΛHT2 conformer undergoes conformational changes in preference to the 5′-G* residue. Consequently, we can now modify the standard general scheme relating the conformers (Figure 1) to that shown in Figure S7.

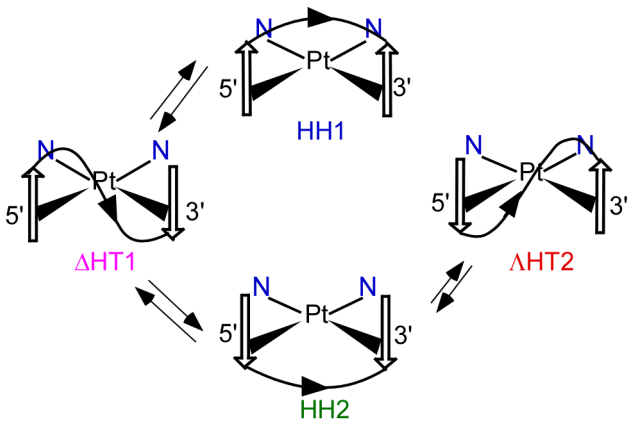

Figure S7. Scheme relating the conformers of an (**R$_4$dt**)Pt(d(G*pG*)) adduct, modified from Figure 1 to show likely pathways. Depicted here are fast interconversion (long counter-parallel arrows) between

the two HH conformers and the ΔHT1 conformer and slow interconversion (short counter-parallel arrows) between the HH2 conformer and the ΛHT2 conformer.

References

1. Marzilli, L. G.; Saad, J. S.; Kuklenyik, Z.; Keating, K. A.; Xu, Y. *J. Am. Chem. Soc.* **2001**, *123*, 2764-2770.
2. Marzilli, L. G.; Ano, S. O.; Intini, F. P.; Natile, G. *J. Am. Chem. Soc.* **1999**, *121*, 9133-9142.
3. Ano, S. O.; Intini, F. P.; Natile, G.; Marzilli, L. G. *J. Am. Chem. Soc.* **1998**, *120*, 12017-12022.
4. Sullivan, S. T.; Ciccarese, A.; Fanizzi, F. P.; Marzilli, L. G. *J. Am. Chem. Soc.* **2001**, *123*, 9345-9355.
5. Mukundan, S., Jr.; Xu, Y.; Zon, G.; Marzilli, L. G. *J. Am. Chem. Soc.* **1991**, *113*, 3021-3027.
6. van der Veer, J. L.; van der Marel, G. A.; van den Elst, H.; Reedijk, J. *Inorg. Chem.* **1987**, *26*, 2272-2275.
7. Williams, K. M.; Cerasino, L.; Natile, G.; Marzilli, L. G. *J. Am. Chem. Soc.* **2000**, *122*, 8021-8030.